Modeling Dynamic Uncertainty in Robot Motions

Aleksandar Timcenko Peter Allen
Center for Research in Intelligent Systems
Department of Computer Science
Columbia University, New York NY 10027 *

Abstract

This paper offers a new method for modeling uncertainties that exist in a robotic system, based on stochastic differential equations. The benefit of using such a model is that we are then able to capture in an analytical structure the ability to properly express uncertainty within the motion descriptions and the dynamic, changing nature of the task and its constraints. With respect to the dynamic nature of robotic motion tasks, the model of the environment uncertainty that we propose here is "dynamic" rather than "static"; the amount of knowledge about the environment is allowed to change as the robot moves. These results suggest that computational models traditionally found in the "lower" levels in robot systems may have application in the "upper" planning levels as well. We also present some experimental results using the model.

1 Introduction

Dealing with uncertainty is one of the major problems in robotics and one of the main obstacles to populating the world with robots that *do something useful*. Some well known motion planning techniques, such as the potential-field method, assume that a robot's sensing, control and knowledge of an environment are perfect. This assumption, albeit never absolutely true, is realistic in non-cluttered environments when the required accuracy in the goal is not critical. The simple — and usually quite sufficient — approach is to slightly "grow" the obstacles and "shrink" the goal in the configuration space to compensate for all present uncertainties. Motions planned under these assumptions are usually called *gross* motions.

Nevertheless, the necessity for a more elaborate treatment of uncertainties exists. Intuitively, by conservatively "growing" the obstacles we may either run out of free space or the goal region may disappear. Thus, we need a planning methodology capable of coping with inherent uncertainties in a more elaborate way. More precisely, we need a tool that allows us to suppress the unwanted effects of different uncertainties — for example, even if our robot "slips" from the prescribed trajectory, we want to be able to guide it towards the goal anyway. Another problem we find is that uncertainties are dynamic; they change over time and position, and we need a mechanism that is capable of expressing and reasoning about time dependent uncertainty. Planning in the presence of uncertainties also poses one additional problem, and that is *recognition* of the goal. Due to sensing inaccuracies, the robot may not be able to recognize that the goal has been attained. The planning system has to make sure that its termination predicate is "strong" enough to prevent getting to the goal without recognizing it.

This paper offers a new method for modeling uncertainties that exist in a robotic system, based on stochastic differential equations. The benefit of using such a model is that we are then able to capture in an analytical structure some key points underlying robot motion: the ability to properly express uncertainty within the motion descriptions, and the dynamic, changing nature of the task and its constraints. Is it possible to exploit the smooth, differentiable topological structure of configuration space and populate it with mathematical entities that lead to plans as solutions of certain differential equations? We may ask if it is possible to use the *predictive* strength of analytical models instead of more traditional search techniques. These are the questions we want to address in our future work, and this paper offers some evidence that they may have positive answers.

We have performed experiments that attempt to quantify the uncertainty in robotic motion control and show how it can be used within our model. The statistical justifiability of the proposed model indicates that it resembles the real nature of the random phenomena that govern the system quite well. More importantly, the method we are about to present offers a way of estimating the variance of different types of uncertainties, thus answering questions about both the qualitative and quantitative nature of uncertainty.

With respect to the dynamic nature of robotic motion tasks, the model of the environment uncertainty that we propose here is "dynamic" rather than "static". That means that the amount of knowledge about the environment is allowed to change as robot moves. If the environment model is built on-line using a robot's sensors, it is natural to assume that the knowledge about the nearby, local neighborhood is more accurate than the knowledge about distant objects. This kind of behavior can be modeled through stochastic differential equations. Since the acquisition of environment models is computationally costly, the increasing variance of a model's uncertainty can be used as a criterion for reexamining the environment and rebuilding its model. This model provides great generality in representing environmental uncertainties.

Significant work in robotic planning in the presence of uncertainties has been done by Lozano-Pérez and colleagues [7, 3, 1]. It recognizes three main sources of uncertainties present in robotic tasks [1, 5]:

- *sensor uncertainty*, caused by imperfection of the sensory equipment
- *control uncertainty*, caused by an imperfection of the control

*This work was supported in part by DARPA contract DACA-76-92-C-007, NSF grants IRI-86-57151, CDA-90-24735, North American Philips Laboratories, Siemens Corporation and Rockwell International.

system

- *environment uncertainty*, caused by the inaccuracy of the world description at the system's disposal

Sensor uncertainty is caused by the imperfection of the sensory system. The first question in "sensory integration" is, according to [5], to identify what is being observed and how accurate those observations are.

The model of sensor uncertainty, as given in [8], is the ball $S(\mathbf{q}_0^0, \varepsilon_{\mathbf{q}_0^0})$ in the configuration space $\mathcal{C}$, centered in the actual position $\mathbf{q}_0^0$ and with the radius $\varepsilon_{\mathbf{q}_0^0}$. It defines the set of possible measurements of a robot's position $\mathbf{q}_0^c$ by its sensors. Mathematically, this can be expressed as $\mathbf{q}_0^c \in S(\mathbf{q}_0^0, \varepsilon_{\mathbf{q}_0^0})$. In the language of probability theory, $\mathbf{q}_0^c$ is the random variable whose probability distribution is bounded around $\mathbf{q}_0^0$ and with the radius $\varepsilon_{\mathbf{q}_0^0}$ — that is, $\mathbf{q}_0^c \sim \mathcal{U}(\mathbf{q}_0^0, \varepsilon_{\mathbf{q}_0^0})$ where $\mathcal{U}$ denotes a bounded but othervise unknown distribution. The probability distribution density function $\psi_{\mathbf{q}_0^c}$ of $\mathbf{q}_0^c$ can be expressed as

$$\psi_{\mathbf{q}_0^c}(\mathbf{q}) = \begin{cases} > 0, & \|\mathbf{q} - \mathbf{q}_0^0\| \leq \varepsilon_{\mathbf{q}_0^0} \\ 0, & \|\mathbf{q} - \mathbf{q}_0^0\| > \varepsilon_{\mathbf{q}_0^0} \end{cases}$$

In sensor system-oriented robotics literature more elaborate models of sensor uncertainties can be found. The generalization of the aforementioned model that we will adopt henceforth will entail an arbitrary probability density function $\psi_{\mathbf{q}_0^c}$.

The usual model of the control uncertainty is the "uncertainty cone" [8, 3]. It is assumed that the *effective* commanded velocity $\mathbf{v}^m$ lies inside the ball with the radius $\varepsilon_{\mathbf{v}^c}$ centered in the *desired* commanded velocity $\mathbf{v}^c$. Since the position $\mathbf{q}_t^m$ in the configuration space $\mathcal{C}$ is given as an integral of the velocity, $\mathbf{q}_t^m = \int \mathbf{v}^m dt$, it turns out that the effective positions conveyed to the robot controller lie inside the *velocity cone*, denoted $B(\mathbf{q}_0^c, \mathbf{v}^c, \varepsilon_{\mathbf{q}_0^c})$. Notation $B(\mathbf{q}_0^c, \mathbf{v}^c, \varepsilon_{\mathbf{q}_0^c})$ stands for a cone with an apex in $\mathbf{q}_0^c$, a principal axis in direction $\mathbf{v}^c$ and a central angle in the apex of $2 \arcsin \varepsilon_{\mathbf{q}_0^c}$. The apex of the cone is placed in the initial position $\mathbf{q}_0^c = \mathbf{q}_0^m$.

The important underlying assumption in the "velocity cone" model is that the probability distribution inside the cone is bounded, meaning that all directions inside the cone are possible, and that directions outside the cone are impossible. This is an approximation which has its foundations in its simplicity and efficiency in modeling the uncertainty.

Although the assumption that the planner possesses the complete knowledge about the environment is for all but the most simple tasks unrealistic, the modeling of uncertainties present in the environment description that is at the system's disposal has received relatively little attention. This fact is probably due to the intrinsic difficulties in introducing randomness in geometrical descriptions of the environment. Although sometimes used, the terms "uncertain geometry" or "probabilistic geometry" are not adequate notation for the set of tools that are needed for these purposes, mainly because they refer to branches of mathematics that are inherently ill-defined (cf. Bertrand's paradox[1]). Nevertheless, there have been some noteworthy attempts to theoretically address model uncertainties [2, 1].

[1] The probability that a chord randomly drawn in a circle is longer than circle's radius depends on the way we define random drawing. This ambiguity is called Bertrand's paradox.

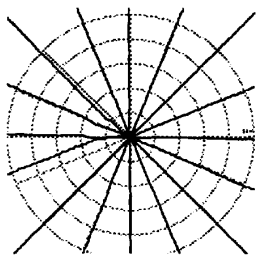

Figure 1: Motions in different directions. Black lines represent observed positions of the pointing device. Gray lines are desired trajectories. Concentric circles are drawn with 1 inch increments in radius. The displacements from the ideal (desired) trajectories are measured along those circles.

2 An Uncertainty Model Based On Stochastic Differential Equations

The guiding idea in this work was to find a unifying model of all three types of uncertainties that is expressive enough to accommodate for most observed phenomena, yet manageable so that it can be used as a basis for motion planning. We propose a model based on stochastic differential equations, developed in the remaining part of this section. This model is a generalization of the "classical" uncertainty model (which is based on uniformly distributed random variables).

In the next few paragraphs, we will adopt the model for sensor uncertainty, explain the experiment that has been conducted in order to retrieve the nature of the control uncertainty, model that uncertainty by a stochastic differential equation, verify the model and estimate its parameters through a statistical test, and present the environment model of the same type.

For the purposes of this paper, we will assume sensor uncertainty is modeled by a known distribution function $\psi_{\mathbf{q}_t^c}$. Due to its simplicity, the common approximation of ψ is a Gaussian distribution:

$$\psi_{\mathbf{q}_t^c}(\mathbf{q}) = \frac{1}{(2\pi)^{n/2}(\det\Sigma^c)^{1/2}} e^{-(\mathbf{q}-\mathbf{q}_t^0)^T(\Sigma^c)^{-1}(\mathbf{q}-\mathbf{q}_t^0)/2}$$

where n is the dimensionality of the configuration space (i.e. the dimensionality of $\mathbf{q}$) and Σ^c is the covariance matrix. We will mainly address the simple case of diagonal covariance matrix, $\Sigma^c = \mathrm{diag}(\sigma^{c2} \ \ldots \ \sigma^{c2})$.

Characterizing the actual sensor error is a difficult and important problem that is the subject of ongoing research (see, for example, [5]).

Before we develop the model of the control uncertainty, we will present an experiment that was used to analyze its nature. It will turn out that the measured data comply to the theoretical model in a statistical test that we have conducted. That implies that our model accurately describes the random phenomenon of control uncertainty.

The experimental setup for investigating the nature of the control uncertainty was as follows. A Sun workstation pointing device

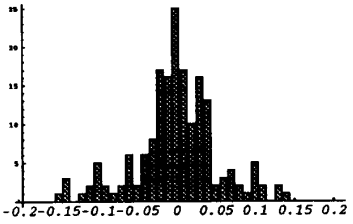

Figure 2: Histogram of the radial displacements of the observed points from the ideal points in all 16 directions, over all experimental runs. The trajectory was 5 inches long. Horizontal axis represents the displacement in inches, and vertical the cumulative number of points in 0.005 inch wide buckets. The total number of points is 240 (15 runs, each contributing 16 points).

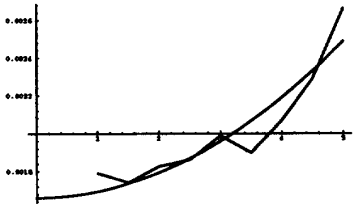

Figure 3: The variances of measured data versus the least-square fit of the parabola. The horizontal axis denotes the distance traveled in inches and the vertical axis is the variance in inches squared.

("mouse") was placed in the gripper of a PUMA-560 and positioned directly above the mouse pad. The dimensions of the mouse pad were approximately 6 by 8 inches. Straight-line motion in the xy plane was commanded in 16 different directions, with angular differences of $\pi/8$ radians. The length of each motion was approximately 5 inches. Figure 1 shows one example run. Black lines represent actually observed motion of the pointing device, while gray lines are ideal desired trajectories. Concentric circles are drawn for reference. The experiment has been conducted several times in three different positions: close to the inner boundary of the work space, in the middle of the work space and close to the outer boundary of the work space. The displacements from the ideal trajectory are registered for each commanded direction for different trajectory lengths. The histogram of the displacements in all directions for the 5 inch trajectory length are given in figure 2. This figure indicates that the nature of the random displacements is Gaussian rather than uniform. Secondly, we have experimentally observed that the variances of the displacements increases with the trajectory length. This observation, combined with the similar observations for other trajectory lengths, leads us to make the following two hypotheses:

- the control uncertainty is modeled by a normal distribution
- the variance of the displacements introduced by the control uncertainty rises with the trajectory length

From the modeling perspective, there are several reasons for these assumptions. Firstly, the Gaussian distribution is a solution of the linear stochastic differential equation with constant coefficients. In that sense, that is the simplest possible case. Secondly, the changing variance assumption is, as stated in the introduction, a phenomenon that exists in both control and environment uncertainties. Rephrased, the two assumptions from above may read as follows: our model should be as simple as possible (i.e. linear with constant coefficients) and should model the phenomena we have observed (i.e. the increasing variance). The next sections formulate the model and measure how well it agrees with some robotic motion tasks.

Let the control uncertainty be modeled by a stochastic differential equation

$$\mathbf{dq}^m = \mathbf{dq}^c + \Sigma^m \mathbf{d}W^m \tag{1}$$

Let us try to justify this model. We have assumed earlier that the velocity $\mathbf{v}^m$ lies inside the sphere centered in $\mathbf{v}^c$. Now we will reformulate that assumption: let $\mathbf{v}^m$ be a random variable obtained by superimposing additional noise on $\mathbf{v}^c$:

$$\mathbf{v}^m = \mathbf{v}^c + W \tag{2}$$

where W is the noise component (a Wiener random process). Since $\mathbf{v}^m = \dot{\mathbf{q}}^m$ and $\mathbf{v}^c = \dot{\mathbf{q}}^c$ (dot denotes time differentiation) after multiplying the left and right side of 2 by $\mathbf{d}t$, it becomes

$$\mathbf{dq}^m = \mathbf{dq}^c + \Sigma^m \mathbf{d}W^m$$

where W^m is another Wiener process (appropriately scaled so that it has correct dimensionality) and Σ^m is a constant that determines the amount of noise in the mapping from $\mathbf{q}^c$ into $\mathbf{q}^m$. In their full generality, W^m is a matrix and Σ^m is 3-dimensional object (tensor) that "contracts" a matrix into a vector. In order to simplify the following analysis, we will consider Σ^m and W^m to be diagonal. This approximation breaks the interdependencies between different coordinates and resolves equation 1 into a set of n scalar equations (n is the dimension of the configuration space). The experiment we have conducted supports this assumption. Nevertheless, it may be interesting to examine the model in its full generality.

The type of solution of equation 1 we are interested in is a probability density function $\psi_{\mathbf{q}_t^m}$ of the random variable $\mathbf{q}_t^m$. It can be shown [11, 4] that $\psi_{\mathbf{q}_t^m}$ is the solution of the Kolmogorov (backward or forward) equation of the form[2]

$$\psi_{q_t^m}(q) = \frac{1}{2\pi\sigma^m(q_t^c - q_0^c)} \mathrm{e}^{-\frac{(q-q_0^c)^2}{2\sigma^{m2}(q_t^c - q_0^c)}} \tag{3}$$

Thus, q_t^m is normally distributed, $q_t^m \sim \mathcal{N}\left(q_t^c, \sigma^{m2}(q_t^c - q_0^c)\right)$, with expectation q_t^c and variance $\sigma^{m2}(q_t^c - q_0^c)$. This means that as the robot moves further from the initial point, the uncertainty of

[2] We have dropped boldface to denote scalar values. $(\sigma^m)^2$ is the appropriate diagonal element of Σ^m.

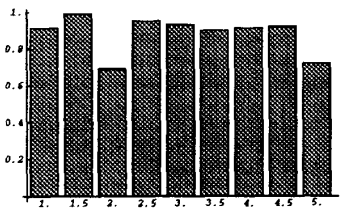

Figure 4: The confidence levels for distribution fits for all observed distances. Horizontal axis is the distance traveled in inches and the vertical axes is the confidence level obtained by a χ^2 test.

its position increases. This is intuitively expected and we wish to incorporate this idea in our model. The reason for introducing a stochastic equation rather than a static probability distribution is to include dynamically changing uncertainty.

The model derived in the previous paragraph was tested against the experimentally obtained data. We have assumed that the discretization error introduces additional Gaussian noise with the covariance matrix Σ^c. Knowing that the summation of two Gaussian random variables results in another Gaussian variable with a variance equal to the sum of the variances of addends, by combining Σ^c with the relation 3 we obtain the theoretical model for the variance Σ_t^m of the measured data:

$$\Sigma_t^m = \Sigma^c + \Sigma^m(\mathbf{q}_t^c - \mathbf{q}_0^c) \tag{4}$$

The exact numerical interpretation of this equation depends on the particular coordinate frame higher-dimensional objects (such as vectors and matrices) are presented in. We have assumed that there is no interconnections between different coordinates, so the previous equation can be interpreted as a set of n scalar equations of the form

$$\sigma_t^{m2} = \sigma^{c2} + \sigma^{m2}(q_t^c - q_0^c) \tag{5}$$

where σ_t^{m2}, σ^{c2} and σ^{m2} are diagonal elements of Σ_t, Σ^c and Σ^m, respectively. Note that $\Sigma_0 = \Sigma^c$. Figure 3 shows the measured variances (computed by the formula $\mathbf{E}(q_t^{m2}) - (\mathbf{E}q_t^m)^2$) versus the least-square fit of the parabola of the form 5. Figure 4 shows the χ^2 test of the hypothesis that the data are modeled by normal distributions with zero mean and variance given by 5. The statistics are significant in two cases (2in and 5in) and insignificant in all other cases with a confidence level of 0.9.

This statistical analysis shows that the model in 1 accurately represents the random phenomena during robot motion. It also gives a method of quantitatively estimating the parameter σ^m. In this case, $\sigma^m = 3.3 \times 10^{-5}$in. In the next section we show how to use this model for planning purposes.

The environment uncertainty can also be modeled in a similar way to the control uncertainty, which forms part of our overall unifying uncertainty structure. The major difference between the control and environment uncertainty is that the environment uncertainty is a function of the robot's current position. This means that the variance of the model uncertainty varies as the knowledge about the environment varies. This can cause some problems in solving the equations, but there are theoretical methods available to solve for the functional relation between position and variance.

The environment uncertainty, in accordance to relation 1, can be modeled by a stochastic differential equation

$$\mathrm{d}\mathbf{q}^w = \mathrm{d}\mathbf{q}^m + \Sigma^w(\mathbf{q}_t^m)\mathrm{d}W^w \tag{6}$$

where W^w is a Wiener process and $\Sigma^w(\mathbf{q}_t^m)$ is the function of the position $\mathbf{q}_t^m$ that describes the amount of model "noise" in any given point.

Putting together all three components of the uncertainty model, we obtain the following stochastic system:

$$\begin{aligned} \mathrm{d}\mathbf{q}_t^w &= \mathrm{d}\mathbf{q}_t^m + \Sigma^w(\mathbf{q}_t^m)\mathrm{d}W^w \\ \mathrm{d}\mathbf{q}_t^m &= \mathrm{d}\mathbf{q}_t^c + \Sigma^m\mathrm{d}W^m \\ \mathrm{d}\mathbf{q}_t^c &= \mathrm{d}\mathbf{q}_0^c = \mathbf{v}^c\mathrm{d}t \end{aligned}$$

where $\mathbf{v}^c$ is the nominal (commanded) velocity. The initial conditions are:

$$\begin{aligned} \mathbf{q}_0^c = \mathbf{q}_0^m &\sim \mathcal{N}(\mathbf{q}_0^0, \Sigma^c) \\ \mathbf{q}_0^w &\sim \mathcal{N}(\mathbf{q}_0^0, \Sigma_0^w) \end{aligned}$$

Thus, the overall uncertainty model is defined by three constant quantities ($\Sigma^m, \Sigma^c, \Sigma_0^w$) and one function that describes the environment uncertainty (Σ^w). A point in the configuration space is thus represented by a random vector with Gaussian distribution. We will call this model "the continuous uncertainty model".

The objective in developing this model was to capture the dynamic nature of control uncertainty in a comprehensive system that consistently incorporates other types of uncertainties. The method we presented here is an initial step towards estimating a system's uncertainties and using them in motion planning.

3 The Insertion Task in the Continuous Uncertainty Framework

The problem of robotic insertion of a peg in a tight hole is one of the classical tasks both in research and applications. Its importance stems from the fact that numerous assembly procedures can be disassembled into variations of an insertion task. Some estimates mention that over 35% of all assembly tasks are peg insertions and its derivatives. On the other side, its attractiveness for the research community is mainly based on the challenges it poses to the robot controller. The traditional positional control is usually not powerful enough for successful completion of peg insertion, specially in low-tolerance cases. The methods of *compliant motion* have been devised in order to augment a robot's ability to accurately position, resulting in successful insertions with very low clearances [10].

In this section we will apply the continuous uncertainty model, described in the previous section to a peg-in-hole planning task. The planning problem we consider is the following (see figure 5). Let $\mathcal{C}$ be two-dimensional configuration space that consists of a free space $\mathcal{C}_f$ and a polygonal obstacle $\mathcal{CB}$. As we will see, the requirement that the configuration space is two-dimensional is not essential for the planning algorithm that we will present and stems mainly from

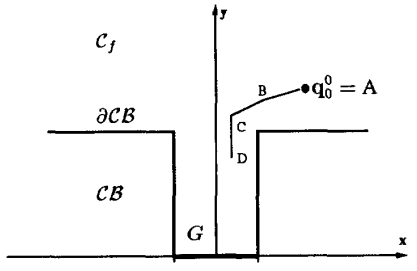

Figure 5: The task is to get to the goal region G starting from $\mathbf{q}_0^0$.

the ease of visualization. There are two types of motion allowed: "free-flying" motion through the interior of $\mathcal{C}_f$ and the compliant motion along the obstacle's boundary $\partial\mathcal{CB}$. The usual way to model the compliant motion is to assume that robot's controller behaves as a *generalized damper* [9]. The generalized damper guarantees that upon contact the motion resumes in directions orthogonal to the direction of a reactive force. The friction force is modeled by a "friction cone" [8, 3] and there are two possible outcomes upon the impact with an obstacle: the robot either "sticks" and stops (if the velocity points inside the velocity cone) or slides along the obstacle. The task is as follows: starting from the initial configuration $A = \mathbf{q}_0^0 \in \mathcal{C}_f$, plan the trajectory so that it ends by sticking on a given edge (goal edge, denoted G) from the obstacle's boundary $\partial\mathcal{CB}$ (see figure 5). The known parameters that model the environment are: the friction coefficient μ, the sensor uncertainty σ^c and the control uncertainty σ^m. The result of the planning process should be the sequence of points $B, C, D, \ldots$ For now, we will assume that the environment uncertainty does not exist (we hope to address this issue in future research).

The robot's position at time instant t is modeled by a random variable $\mathbf{q}_t^m$ that has a Gaussian distribution with the mean $\mathbf{q}_t^0$ and the covariance matrix Σ_t. The covariance matrix is given by relation 4.

Let us examine the possible interrelations between $\mathbf{q}_0^m$ and $\mathbf{q}_t^m$. At time instant 0 the robot is still in the free space $\mathcal{C}_f$, in point $\mathbf{q}_0^m$. The contact with an obstacle hasn't occurred yet. After the time interval t the robot is, due to the combined effect of sensor and control uncertainty, in a random point $\mathbf{q}_t^m$. We want to choose $\mathbf{v}_t^c$ such that the expected position at time instant t (that is $\mathbf{q}_t^0$) has certain desirable properties. The criterion we propose here for the choice of $\mathbf{v}_t^c$ is following:

> *Choose $\mathbf{v}_t^c$ so that if the impact with an obstacle occurs during the move from $\mathbf{q}_0^m$ to $\mathbf{q}_t^m$ the probability that the resulting compliant motion will be either sticking in the goal or sliding towards the goal will be maximal.*

If the probability that the "good" compliant motion will occur in the case of impact is considered as a probability that a plan for a given task succeeds, than the requirement above is simply asking for the maximization of the success probability.

We will base the analysis of the success probability on several assumptions:

- The magnitude of the velocity v is constant during the move.
- The motion duration t is long enough so that the probability of an impact with the obstacle is ≈ 1
- The goal region G is simply connected in a sense that if there were no uncertainties there would be a single interval of approach angles $\theta_0 \in [\theta_1, \theta_2]$ that would lead towards the goal.

Having chosen the criterion we want to optimize, we need to express it mathematically. The probability of a success, $\Psi\{\mathsf{success}\}$, can be expressed as a probability that the initial point $\mathbf{q}_0^m$ is in free space $\mathcal{C}_f$ and the end point $\mathbf{q}_t^m$ is inside the part of the obstacle $\mathcal{CB}_S(\mathbf{q}_0^m)$ that results in sliding motion towards the goal. The obstacle $\mathcal{CB}$ can be divided into two subsets

$$\mathcal{CB} = \mathcal{CB}_S(\mathbf{q}_0^m) \cup \mathcal{CB}_F(\mathbf{q}_0^m)$$

The set $\mathcal{CB}_S(\mathbf{q})$ is the set of configurations $\mathbf{q}' \in \mathcal{CB}$ such that if the motion starts in $\mathbf{q}$ and it is aimed towards $\mathbf{q}'$, the compliant motion after collision (which is inevitable since the path $\overline{\mathbf{qq}'}$ intersects the obstacle boundary $\partial\mathcal{CB}$) results in either sticking in the goal or sliding towards the goal (S in the subscript of $\mathcal{CB}_S$ stands for "success"). Analogously, the set $\mathcal{CB}_F(\mathbf{q})$ is the set of configurations $\mathbf{q}' \in \mathcal{CB}$ such that, on the path from $\mathbf{q}$ towards $\mathbf{q}'$, the resulting compliant motion results either in sticking outside the goal or sliding away from it (the subscript F in $\mathcal{CB}_F$ stands for "failure").

Now the success probability $\Psi\{\mathsf{success}\}$ can be written as

$$\Psi\{\mathsf{success}\} = \Psi\{\mathbf{q}_0^m \in \mathcal{C}_f \wedge \mathbf{q}_t^m \in \mathcal{CB}_S(\mathbf{q}_0^m)\} \tag{7}$$

Note that the set $\mathcal{CB}_S(\mathbf{q}_0^m)$ of "good" end points $\mathbf{q}_t^m$ depends on the point $\mathbf{q}_0^m$.

We already have distribution density functions of $\mathbf{q}_0^m$ and $\mathbf{q}_t^m$ (relation 3). If we substitute them in relation 7 we get

$$\Psi\{\mathsf{success}\} = \int_{\text{lines that lead to goal}} \text{density} = \int_{\mathbf{p}_i \in \mathcal{C}_f} \int_{\mathbf{p}_j \in \mathcal{CB}_S(\mathbf{p}_i)} \psi_{\mathbf{q}_0^m}(\mathbf{p}_i)\psi_{\mathbf{q}_t^m}(\mathbf{p}_j)\mathrm{d}\mathbf{p}_i\mathrm{d}\mathbf{p}_j \tag{8}$$

This integral can be computed using appropriate numerical technique. We have used Monte-Carlo integration because it is well-suited for integrating over irregular regions. Figure 6 presents the success probability computed for series of approach angles θ between -1.5 rad and -2.8 rad. The number of points used in the Monte-Carlo integration was 1000. The other parameters had values $\sigma^c = 0.1, \sigma^m = 0.03, v = 1, t = 1$.

The success probability $\Psi\{\mathsf{success}\}$ is the function of the approach angle θ. The optimal approach angle θ^* is the one that results in the maximal value for the success probability. One possible approach to planning is to maximize Ψ as a function of θ using some numerical method. Figure 6 indicates that we have to apply some kind of search strategy in order to find the optimal value for θ (which in figure 6 would intuitively be around -2.2 rad, i.e. in the middle of the interval of high success probabilities). Especially for the case of low uncertainties, the shape of the curve in figure 6 tends to be rectangular thus virtually eliminating analytical techniques for finding the

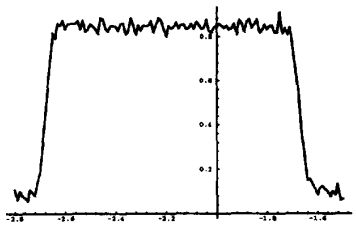

Figure 6: The success probability Ψ (y axis) for various approach angles θ (x axis) for the peg-insertion task in figure 1

maximum of a function. This can be costly since the computation of Ψ for each θ involves evaluation of a double integral in 8.

The alternative approach is to take advantage of the fact that Ψ is periodic in θ and to look for the maximum of the first harmonic of its Fourier series expansion. The main waveform of Ψ can be approximated by the first harmonic in its Fourier expansion. Under the assumption that the goal region is simply connected, the position of maximum of the first harmonic is given by the argument of the coefficient c_1. Thus, in order to compute the optimal approach angle θ^* one needs only to compute the coefficient c_1 of Ψ's Fourier transform. The advantage is that the complexity of computing c_1 is of the same order as the complexity of computing Ψ, while any numerical technique for finding maximum would involve numerous evaluations of Ψ, which is costly. The Fourier coefficient c_1 can be computed relatively straightforwardly in the closed form. It can be shown that c_1 can be expressed in the form

$$c_1 = K \int_{\mathbf{p}_i \in C_f} \psi_{\mathbf{q}_f^m}(\mathbf{p}_i) d\mathbf{p}_i \int_{\substack{\theta \text{ leads to} \\ \text{the goal from } \mathbf{p}_i}} e^{-i\theta} d\theta$$

where K is a constant and the integration in θ is done over all approach angles that lead towards the goal from $\mathbf{p}_i$. Note that here the requirement about the simple connectivity of the interval of "good" angles is not necessary. The optimal approach angle is given by the argument of c_1: $\theta^* = \arg c_1$. The complexity of calculating θ^* is NG, where N is the number of points in Monte-Carlo integration in $\mathbf{p}_i$ and G is a measure of geometrical complexity of the environment (i.e. the complexity of computing the integral in θ).

In the configuration space of dimension n the approach direction is a vector in $n(n-1)/2$-dimension manifold [6]. Since we need to compute a Fourier series expansion for each direction coordinate, that implies that the complexity would be of order n^2NG. The validity of this approach still has to be experimentally verified in the multidimensional case, but it seems that it is a tractable problem.

4 Conclusion

In this paper we have developed a new method for modeling uncertainties in robotic systems and demonstrated its applications on a simple planning task. Our uncertainty model is based on stochastic differential equations and continuous probability distributions. All three types of uncertainties present in a robotic system — sensor, control and environment — can be modeled using the same principle, thus allowing the unified approach to planning of robot motions.

The general environment model is another topic that we consider as a contribution of this paper. Since all three types of uncertainties are encompassed in one unifying system of stochastic equations, the treatment of environment uncertainty is not any different than the treatment of other two types of uncertainty. Besides that, the recognition of the need for varying amounts of environment uncertainty allows for modeling the environments where the amount of knowledge changes as a function of a current position.

We have implemented and experimented with the simple task that involves uncertainty: peg-in-hole insertion planning with a constant velocity in the presence of control uncertainty. The planning is based on the continuous uncertainty model . This approach lets us define the concept of success probability and use it as the optimization criterion. The method we have used for optimization of the success probability was analytical, demonstrating the applicability of these types of methods to problems where discrete search techniques have been utilized. Nevertheless, the quest for global extremum of an analytical function is genuinely a search process. It seems that the very nature of the planning problem requires a certain type of search procedure to take place, since in this case we have replaced search in a discrete space with search in the space of continuous analytic functions. However, there are indications that that replacement may lead to more efficient algorithms, specially in multidimensional or cluttered environments.

We hope that this research effort will result in an comprehensive system for planning tunable parameters of robotic tasks in the presence of uncertainty. There are however many issues that need to be addressed in the future work. The theoretical model developed in this paper shows promises that it can be used as a basis for the future motion planning system.

References

[1] B. R. Donald. *Error Detection and Recovery in Robotics.* Springer-Verlag, 1987.

[2] H. F Durrant-Whyte. Uncertain geometry in robotics. In *Proceedings of the IEEE Conference on Robotics and Automation*, pages 851–856, 1987.

[3] M. Erdmann. Using backprojections for fine motion planning with uncertainty. *International Journal of Robotics Research*, 5(1), 1986.

[4] A. Friedman. *Stochastic Differential Equations and Applications.* Academic Press, 1975.

[5] G. D. Hager. *Task-Directed Sensor Fusion and Planning: A Computational Approach.* Kluwer Academic Publishers, 1991.

[6] J.-C. Latombe. *Robot Motion Planning.* Kluwer Academic Publishers, 1991.

[7] T. Lozano-Peréz. Spatial planning: A configuration space approach. *IEEE Transaction on Computers*, C-32(2):108–120, 1983.

[8] T. Lozano-Peréz, M. T. Mason, and R. H. Taylor. Automatic synthesis of fine-motion strategies for robots. *International Journal of Robotics Research*, 3(1):3–24, 1984.

[9] M. T. Mason. Compliance and force control for computer controlled manipulators. *IEEE Transaction on Systems, Man and Cybernetics*, SMC-1(6):418–432, 1981.

[10] D. R. Strip. Insertions using geometric analysis and hybrid force-position control: Method and analysis. In *Proceedings of the IEEE Conference on Robotics and Automation*, pages 1744–1751, 1988.

[11] A. Timcenko and P. Allen. Modeling uncertainties in robot motions. In *Applications of AI to Real-World Autonomous Mobile Robots, AAAI Fall Symposium Series*, 1992.